Huh *et al. Micro and Nano Syst Lett (2017) 5:5*
DOI 10.1186/s40486-016-0038-2

Micro and Nano Systems Letters

LETTER Open Access

Simple and robust resistive dual-axis accelerometer using a liquid metal droplet

Myoung Huh[1], Dong-Joon Won[1], Joong Gil Kim[2] and Joonwon Kim[1*]

Abstract

This paper presents a novel dual-axis accelerometer that consists of a liquid metal droplet in a cone-shaped channel and an electrode layer with four Nichrome electrodes. The sensor uses the advantages of the liquid metal droplet (i.e., high surface tension, electrical conductivity, high density, and deformability). The cone-shaped channel imposes a restoring force on the liquid metal droplet. We conducted simulation tests to determine the appropriate design specifications of the cone-shaped channel. Surface modifications to the channel enhanced the nonwetting performance of the liquid metal droplet. The performances of the sensor were analyzed by a tilting test. When the acceleration was applied along the axial direction, the device showed ~6 kΩ/g of sensitivity and negligible crosstalk between the X- and Y-axes. In a diagonal direction test, the device showed ~4 kΩ/g of sensitivity.

Keywords: Accelerometer, Simple, Robust, Liquid metal droplet, Thermoplastic, Cone shaped channel, Nichrome electrodes

Background

Different types of microelectromechanical systems (MEMS) accelerometers, which are widely used in moving systems (e.g., automotive systems and military weapon systems), have been developed [1–4]. Most of these accelerometers have solid proof mass parts that move with respect to input acceleration. These accelerometers, however, require complex signal processing steps (e.g., amplification, filtering, and conversion). Furthermore, they use a proof mass that is suspended by fixed beams that are complicated to fabricate and may incur mechanical fatigue [5–9].

To increase the simplicity and robustness of the accelerometer, Park et al. developed an accelerometer using a liquid metal (LM) droplet (i.e., mercury) [10]. Because mercury has electrical conductivity (specific electrical resistance: 0.96×10^{-6} Ω m) and high density (~13.5 g/cm^3), Park et al. used mercury as an electrode and proof mass simultaneously. Mercury also has the deformability of liquid, which does not suffer from fatigue. Therefore, the robustness of the device can be improved. This accelerometer, however, measures the acceleration discontinuously and only along a single axis.

In this paper, we introduce a simple and novel method to overcome the disadvantages of previously researched accelerometers that use an LM droplet. Our device consists simply of two components: a cone-shaped channel made of thermoplastic, in which an LM droplet (i.e., mercury) is placed, and an electrode layer with four Nichrome [specific electrical resistance: $(1.0–1.5) \times 10^{-6}$ Ω m] electrodes. Since the resistance of the device changes continuously according to the input acceleration, our device can measure the acceleration continuously. Moreover, the cone-shaped channel and four Nichrome electrodes make it possible to measure dual-axis acceleration.

The accelerometer was successfully fabricated using micromachining techniques. To improve its performance, a cone-shaped channel is designed by simulation tests using the commercially available tool COMSOL Multiphysics. The surface is modified by using a sandblaster to form the microstructures inside the channel to enhance the nonwetting characteristic of the LM droplet. The performance of the fabricated device is analyzed through tilting tests. With these tests, we confirm

*Correspondence: joonwon@postech.ac.kr
[1] Department of Mechanical Engineering, Pohang University of Science and Technology (POSTECH), 77 Cheongam-Ro, Nam-Gu, Pohang, Gyeongbuk 37673, Republic of Korea
Full list of author information is available at the end of the article

that our device can measure the X- or Y-axis (single-axis acceleration) and also the diagonal axis (dual-axis acceleration). The device shows ~6 kΩ/g of sensitivity in the axial direction and ~4 kΩ/g in the diagonal direction.

Device concept and design

Configuration and operational principle

The device consists of two parts: a cone-shaped channel made of thermoplastic, in which LM is placed, and an electrode layer with four Nichrome electrodes (Fig. 1a). Figure 1b shows the fabricated device, in which an LM droplet is used as a proof mass.

As shown in Fig. 1c, in an accelerated state, the induced inertial force moves an LM droplet toward the edge of a channel. On the other hand, the movement of the LM droplet induces an imbalance in the Laplace pressure between one side and the opposite sides of the LM. The imbalance of the Laplace pressure induces a force by which the LM droplet moves toward the center of the channel. For simplicity, "Laplace pressure" has the same meaning as the force by which the LM droplet moves toward the center of the channel in this paper. The LM droplet stops moving when the balance between the inertial force and Laplace pressure are in equilibrium. Generally for electrodes, the resistance is proportional to the electrode length (L) and inversely proportional to the cross-sectional area (A). In our device, the cross-sectional area (A) of the electrodes is constant, but the electrode length (L) changes according to the position of the LM droplet. When the LM moves to the right, the length of the right electrode decreases. In the same manner, the resistance of the right electrode decreases. Since electric current takes the path of least resistance, it prefers to flow through the LM droplet rather than the Nichrome.

Figure 1d shows a schematic of the acceleration sensing mechanism. ΔR_x and ΔR_y are the differences in the resistance between two electrodes along the X-axis and Y-axis, respectively (i.e., $\Delta R_x = R_1 - R_3$ and $\Delta R_y = R_2 - R_4$). As mentioned earlier, the LM droplet moves based on the input acceleration. If acceleration is applied in the direction of the X-axis only, ΔR_x increases. On the other hand, ΔR_y is almost zero since the changes in both resistances along the Y-axis are almost equal.

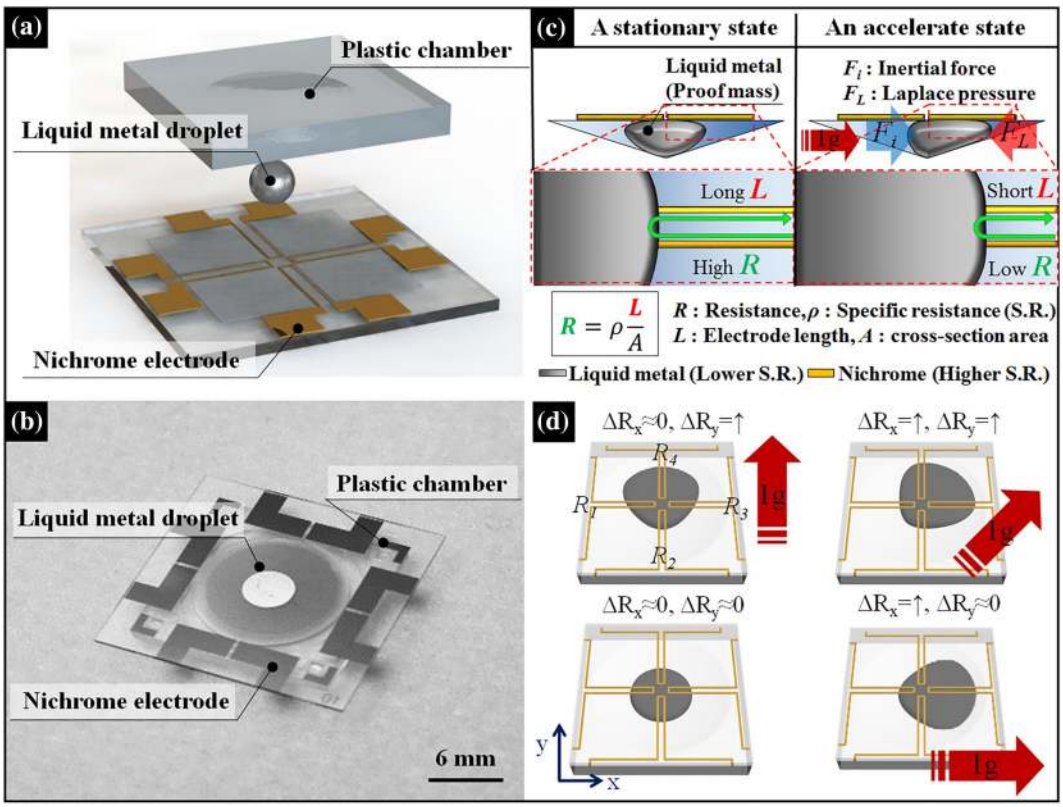

Fig. 1 Design and operating mechanism of dual-axis accelerometer. **a** Schematic of the device. **b** Device image. **c** Acceleration sensing mechanism. Here, ΔR_x indicates the difference in resistance in the direction of the X-axis, and ΔR_y indicates that in the direction of the Y-axis. **d** Principle of resistance change

Design of the channel

As shown in Fig. 2a, the Laplace pressures at the left and right sides in the liquid droplet between two nonparallel plates are determined by a combination of the surface tension (γ) of a liquid droplet, the contact angle (θ), the angle between the two plates (α), and the distance between the apex edge (d_1 and d_2) and the liquid droplet. The liquid droplet between two nonparallel plates moves until the Laplace pressure difference is zero [11, 12]. The surface tension is a property of the LM droplet, and the contact angle is determined by the nature of the contacting materials [13]. Therefore, we cannot control these parameters by designing the channel. The angle of the edge is a main parameter in designing the channel. We choose three designs to control the angle of the cone-shaped channel, as shown in Table 1.

We conduct simulation tests for the three designs using the commercially available tool COMSOL Multiphysics (Fig. 2a). We applied acceleration to the three designs via COMSOL Multiphysics and obtained the distance changes based on the right side of the LM droplet in the channel depending on the given accelerations. Finally, we selected a channel that has 10 mm of diameter and 1 mm of depth since the change in distance of the LM droplet is at its maximum (0.5 mm, 1 g) (Fig. 2b).

Surface modification of channel

An LM droplet performs best as a proof mass when the liquid metal does not exhibit stiction, friction, or any kind of resistance to sensitivity, repeatability, or response time when moving. To facilitate the movement of the LM droplet, we form microstructures uniformly inside the thermoplastic channel by using a sandblaster (20 μm of sand, 0.7 MPa, 5 s) (Fig. 3a).

Table 1 Design parameters of channel

	D (mm)	*h* (mm)	*θ* (°)
Design 1	10	0.5	~5.7
Design 2	10	1	~11.3
Design 3	5	1	~21.8

The scanning electron microscopy (SEM) images of the bare and sandblasted surfaces of thermoplastic are shown in Fig. 3b, c. The sandblasted surface was uniformly covered by microstructures, but the bare surface was smooth. To observe the wettability of the sandblasted and bare surfaces, we measured the contact angle (CA) and the contact angle hysteresis (CAH). The CA between the bare thermoplastic surface and the LM droplet (volume ~1 μL) is ~150°, and the CAH is ~20°. The CA between the modified surface and the LM droplet is ~165°, and the CAH is ~2°. The smaller CAH of the modified surface indicates that the LM droplet moves more easily on the sandblasted surface than on the bare surface.

Fabrication process

Thermoplastic and Nichrome electrode layers are used in our device. The channel was fabricated on a thermoplastic plate. We created a stainless steel 304 mold and fabricated a channel (10 mm in diameter, 1 m in depth) simply by using a hot-embossing process (Fig. 4a, b). The surface was modified by using a sandblaster to form microstructures inside the channel to enhance the nonwetting performance of the LM droplet. An electrode layer was fabricated on a glass substrate by using a lift-off process (Fig. 4c). Nichrome electrodes (thickness of 2000 Å) were deposited by sputtering on an AZ5214E photoresist

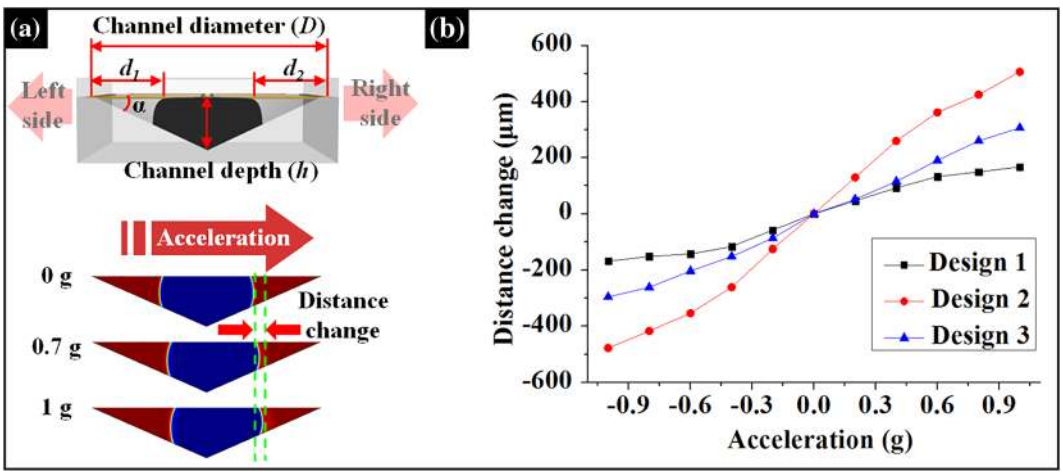

Fig. 2 Channel design. **a** Simulation for three designs using commercially available tool COMSOL Multiphysics. **b** Distance changes of liquid metal droplet caused by input acceleration in three different designs

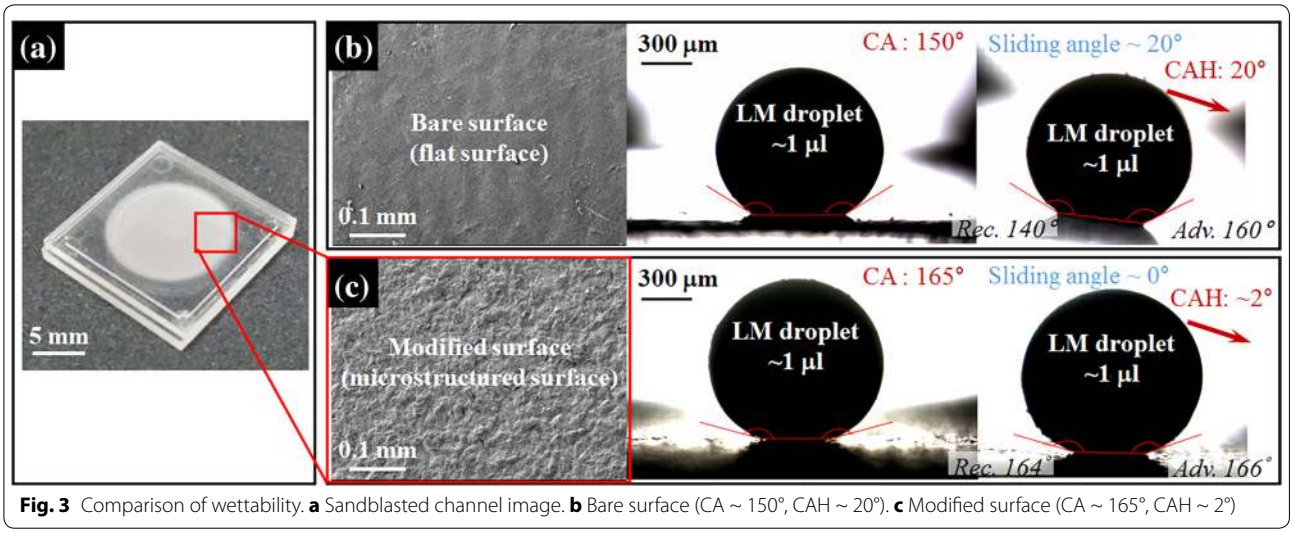

Fig. 3 Comparison of wettability. **a** Sandblasted channel image. **b** Bare surface (CA ~ 150°, CAH ~ 20°). **c** Modified surface (CA ~ 165°, CAH ~ 2°)

(width of 10 μm) patterned glass wafer. Finally, the electrode pattern was achieved by dipping the wafer into an acetone solution. An LM droplet (~10 μL) was placed inside the microstructured channel, and the electrode layer was bonded using ultraviolet (UV) curable adhesive (Fig. 4d).

Results

Experimental setup

We performed a tilting test using a custom-built setup to verify the concept of the proposed dual-axis accelerometer (Fig. 5). The acceleration applied to the device was controlled by a rotary stage, and a digital multimeter (Agilent 34401A) was used to measure the resistance of the four electrodes. LabVIEW was used to control the tilting angle using serial communication, and to calculate the differences in the resistances of the electrodes.

Tilting test

Accelerations ranging from 0 to 1 g were applied to the sensor by controlling the tilting angle. When the accelerometer was vertical with respect to the ground, the acceleration was 1 g. On the other hand, when it was horizontal, the acceleration was 0 g. In Fig. 6, ΔR indicates the difference in the resistances between two electrodes along the X-axis (ΔR_x) and Y-axis (ΔR_y). When the input accelerations were applied along the X- or Y-axis, ΔR was about 6 kΩ at 1 g (Fig. 6a). Here, the interference between the X- and Y-axis was negligible (close to 0 kΩ). When the acceleration was applied in a diagonal direction, the values of ΔR were approximately 4 kΩ at 1 g, which was similar to the magnitude between the X- and Y-axes (Fig. 6b). We confirmed that ΔR in the diagonal acceleration test (~4 kΩ) was less than that of the axial input test (~6 kΩ). The reason is that the part of the LM droplet close to the axis of acceleration showed a tendency to deform more significantly in our channel design. The slopes of the graphs show the sensitivity of the device. The device shows ~6 kΩ/g of sensitivity in the axial direction and ~4 kΩ/g in the diagonal direction.

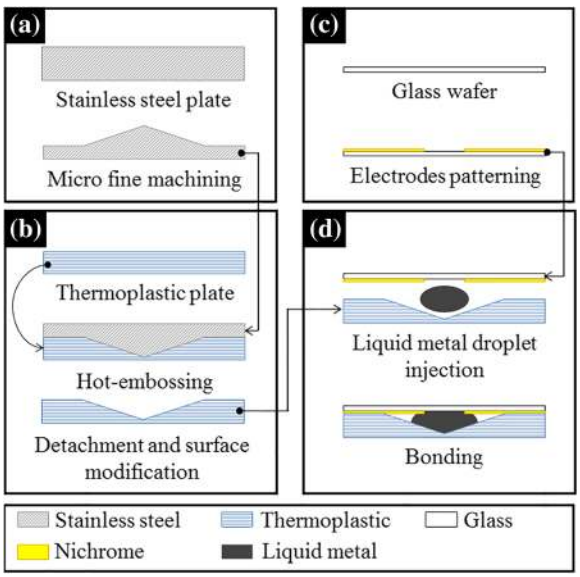

Fig. 4 Fabrication process. **a** Stainless steel mold. **b** Channel (*bottom layer*). **c** Electrodes (*top layer*). **d** Device assembly

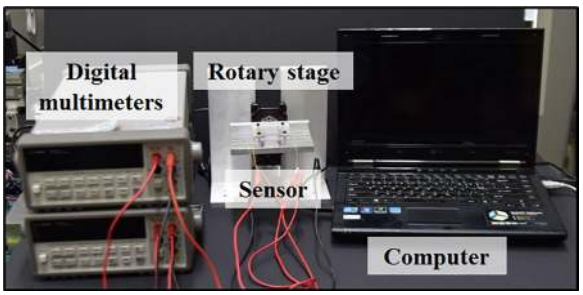

Fig. 5 Experimental setup for tilting test

Conclusion

We developed a simple and robust dual-axis accelerometer. The device consists of two parts: a cone-shaped channel made of thermoplastic, which is filled with an LM droplet, and an electrode layer with four Nichrome electrodes. An LM droplet was used as a proof mass, and the input acceleration was measured by the difference in the resistance between two electrodes along the X-axis and Y-axis. The channel design was achieved using the commercially available tool COMSOL Multiphysics. To enhance the nonwetting performance of the LM droplet, surface modifications were conducted using a sandblaster to form microstructures inside the channel. The performances of the fabricated device were analyzed by tilting tests. From the test, we confirmed that our device can measure the X- or Y-axis (single-axis acceleration) and the diagonal axis (dual-axis acceleration). The device shows ~6 kΩ/g of sensitivity in the axial direction and ~4 kΩ/g in the diagonal direction.

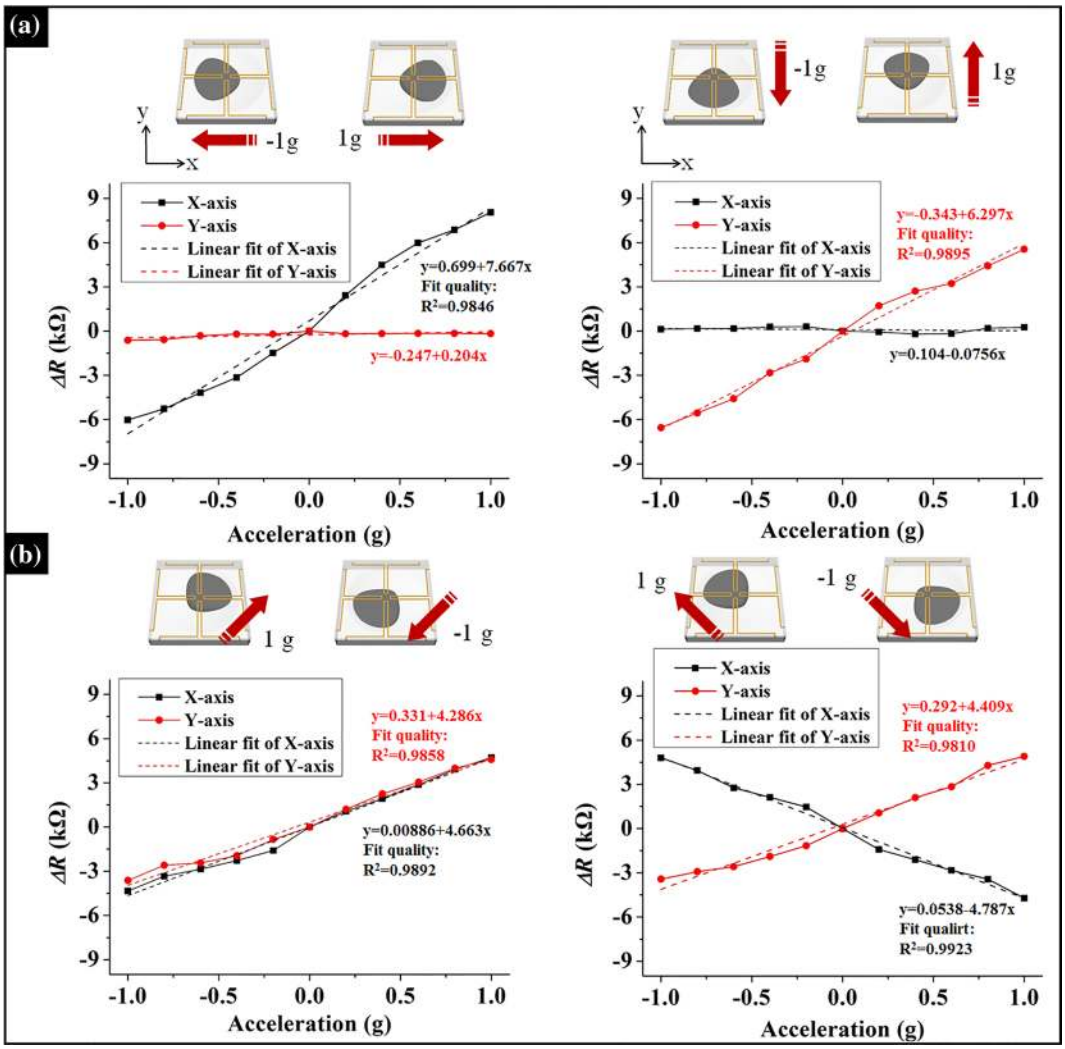

Fig. 6 Results of tilting tests: *ΔR* (total resistance difference of each electrode) of sensor subjected to input accelerations. **a** Input accelerations along X- or Y-axis. **b** Input accelerations with diagonal direction

Abbreviations
MEMS: microelectromechanical systems; LM: liquid metal; SEM: scanning electron microscopy; CA: contact angle; CAH: contact angle hysteresis.

Authors' contributions
MH carried out the experiments, analyzed the experimental result, and drafted the manuscript. D-JW performed the fabrication of device and conducted experiments. JGK and JK carried out experimental measurements and analysis. All authors read and approved the final manuscript.

Author details
[1] Department of Mechanical Engineering, Pohang University of Science and Technology (POSTECH), 77 Cheongam-Ro, Nam-Gu, Pohang, Gyeongbuk 37673, Republic of Korea. [2] Military service in Republic of Korea, Gyeryong-si, Chungcheongnam-do, Republic of Korea.

Competing interests
The authors declare that they have no competing interests.

Funding
This work was supported by the National Research Foundation of Korea (NRF) Grant funded by the Korea Government (MSIP) (No. 2011-0030075).

Received: 7 December 2016 Accepted: 28 December 2016
Published online: 09 January 2017

References

1. Fleming WJ (2008) New automotive sensors—a review. IEEE Sens J 8(11):1900–1921. doi:10.1109/jsen.2008.2006452
2. Khir MH, Qu P, Qu H (2011) A low-cost CMOS-MEMS piezoresistive accelerometer with large proof mass. Sens Basel 11(8):7892–7907. doi:10.3390/s110807892
3. Park U, Rhim J, Jeon JU, Kim J (2014) A micromachined differential resonant accelerometer based on robust structural design. Microelectron Eng 129:5–11. doi:10.1016/j.mee.2014.06.008
4. Mineta T, Kobayashi S, Watanabe Y, Kanauchi S, Nakagawa I, Suganuma E, Esashi M (1996) Three-axis capacitive accelerometer with uniform axial sensitivities. J Micromech Microeng 6(4):431. doi:10.1088/0960-1317/6/4/010
5. Sangkyung S, Jang Gyu L, Byeungleul L, Taesam K (2003) Design and performance test of an oscillation loop for a MEMS resonant accelerometer. J Micromech Microeng 13(2):246. doi:10.1088/0960-1317/13/2/312
6. Aydemir A, Terzioglu Y, Akin T (2016) A new design and a fabrication approach to realize a high performance three axes capacitive MEMS accelerometer. Sens Actuators A Phys 244:324–333. doi:10.1016/j.sna.2016.04.007
7. Tsai M-H, Liu Y-C, Fang W (2012) A three-axis CMOS-MEMS accelerometer structure with vertically integrated fully differential sensing electrodes. J Microelectromech Syst 21(6):1329–1337. doi:10.1109/jmems.2012.2205904
8. Mariani S, Ghisi A, Corigliano A, Zerbini S (2009) Modeling impact-induced failure of polysilicon MEMS: a multi-scale approach. Sens Basel 9(1):556–567. doi:10.3390/s90100556
9. Renuart ED, Fitzgerald AM, Kenny TW, Dauskardt RH (2001) Fatigue processes in silicon MEMS devices. In: Proceedings of the Spring MRS meeting, San Francisco, 18 March 2001. doi:10.1557/PROC-682-N4.8
10. Park U, Yoo K, Kim J (2010) Development of a MEMS digital accelerometer (MDA) using a microscale liquid metal droplet in a microstructured photosensitive glass channel. Sens Actuators A Phys 159(1):51–57. doi:10.1016/j.sna.2010.02.011
11. Prakash M, Quéré D, Bush JWM (2008) Surface tension transport of prey by feeding shorebirds: the capillary ratchet. Science 320(5878):931–934. doi:10.1126/science.1156023
12. Luo C, Heng X, Xiang M (2014) Behavior of a liquid drop between two nonparallel plates. Langmuir 30(28):8373–8380. doi:10.1021/la500512e
13. Blake TD, Bracke M, Shikhmurzaev YD (1999) Experimental evidence of nonlocal hydrodynamic influence on the dynamic contact angle. Phys Fluids 11(8):1995–2007. doi:10.1063/1.870063